Review

Wide-Angle-Tail (WAT) Radio Sources

Christopher P. O'Dea * and **Stefi A. Baum**

Department of Physics & Astronomy, University of Manitoba, 30A Sifton Rd., Winnipeg, MB R3T 2N2, Canada; stefi.baum@umanitoba.ca
* Correspondence: odeac@umanitoba.ca; Tel.: +1-585-309-5713

Abstract: We review the properties of Wide-Angle-Tail (WAT) radio sources. The WAT radio sources are powerful, bent radio sources typically associated with the dominant galaxy in a cluster or group. For the purpose of this review, we define the radio morphology properties of WATs as (1) a sudden jet-tail transition, (2) overall bending of the tails to one side, and (3) non-parallel tails. The mechanism for the rapid jet-tail transition is uncertain but it seems to occur near the transition from the host ISM to ICM. The jet-tail transition may make the jets easier to bend. The narrow range in radio luminosity can be understood if there is a minimum luminosity required to allow the jets to propagate undisturbed for tens of kpc and a maximum luminosity required to allow the jet disruption mechanism to act. WATs are typically hosted by the brightest cluster galaxies in clusters which are currently merging. Thus, WATs can be used as tracers of merging clusters. The merging produces large-scale bulk motions in the ICM which can provide sufficient ram pressure to bend the jets. We suggest that although the Lorentz force may not bend the jets in WATs, it may be relevant in other sources, e.g., protostellar jets.

Keywords: active galactic nuclei; clusters of galaxies; jets; radio sources; wide-angle-tail radio sources

1. Introduction

Clusters of galaxies host radio sources associated with individual galaxies as well as radio emission (relics and halos) specific to the Intracluster Medium (ICM) (for reviews of radio sources in clusters see, e.g., [1,2]). The Wide-Angle-Tail (WAT) radio sources are powerful, bent radio sources that are typically associated with a dominant galaxy in a cluster of galaxies, e.g., [3–5]. As we discuss below, WATs are thought to be produced via the interaction of the outflowing radio jets with the dynamic, magnetized ICM of the cluster. This has three important consequences. (1) WATs can be used to locate clusters of galaxies, e.g., [6–8]. (2) WATs can be used to probe the dynamics of clusters of galaxies, e.g., [9–11]. (3) The bending of the jets can be used to probe the properties of the jets, e.g., [5,12–16]. In order to facilitate research on WATs, we present this review of their properties, environments, and current theories concerning their origin. Here, we only consider sources where the two tails are bent to the same side of the jet ejection direction, i.e., in a "C" or "V" shape. We exclude "Z" or "S"-shaped sources and unbent sources.

In the literature, WATs have been called "bent doubles", "V-shaped" sources, "C-shaped" sources, and "Head-Tail (HT)" sources. However, the class of HT sources includes Narrow-Angle Tail (NAT) sources which are a different type of object, e.g., [17,18]. In this review, we will use the term WATs as suggested by Owen and Rudnick [3]. Further, we note that the literature on WATs does not always define WATs consistently, causing some scatter in the results.

This review is organized as follows. In Section 2, we present the radio properties of WATs. In Section 3, we present the host galaxy properties and environments of WATs. In Section 4, we discuss the various models for WATs. We summarize our thoughts in Section 5.

We define spectral index α such that $S_\nu \propto \nu^\alpha$, where S_ν is flux density at frequency ν.

2. Radio Properties

There are now dozens of WATs with high-quality radio imaging [14,19–29]. There is considerable variation in the radio properties among WATs, likely due to some combination of projection effects, e.g., [30], relativistic beaming, and the complex nature of the interaction of the radio source with the dynamic ICM. Here, we focus on common properties.

2.1. Narrow Range of Radio Luminosity

WATs are known to have a narrow range of radio luminosity of $10^{42} < L_{\mathrm{radio}} < 10^{43}$ ergs s^{-1} integrated over the frequency range 10 MHz to 100 GHz, e.g., [3,25,31,32]. This luminosity range is in the transition between FRI and FRII radio galaxies, e.g., [4,5]. In the current radio source paradigm, there is a relation between radio luminosity and jet properties, e.g., [33–42]. In this paradigm, the lower radio luminosity sources are thought to have weaker radio jets (lower velocity and/or Mach number) which are decelerated on sub-kpc to kpc scales and produce FRI radio sources. The higher radio luminosity sources have more powerful jets that maintain relativistic speeds out to the terminal hot spots and create FRII sources. Consistent with this paradigm, we suggest that there is a minimum radio luminosity required to produce the straight, fast, well-collimated jets that extend to several tens of kpc from the core. Further, we suggest there is a maximum radio luminosity required to allow the jet disruption mechanism to cause the jet-tail transition (Section 4.1).

2.2. Radio Morphology

The large-scale bending of WATs is how they are selected and so this is their defining feature. Figure 1 shows the archetype 3C465. The jets transition abruptly to diffuse tails or plumes (the transition is described in more detail below) after which the tails bend. The tails of a WAT are in general not parallel to each other, but define an angle which is generally between 180° and 90°. The tails are sometimes not straight, but can exhibit additional bending, e.g., the NW tail of 3C465. The gradual, large-scale bending of the tails might be due to buoyancy. As discussed in Sections 2.4.1 and 4.2.2, there is evidence that (1) the jet flow does not persist to the end of the tails and (2) the tails are less dense than the ambient medium, thus making the tails subject to buoyant forces. We can summarize the defining radio morphology properties of WATs as (1) jet-tail transition, (2) overall bending to one side, and (3) non-parallel tails.

One of the striking properties of WATs is the presence of twin jets which are typically narrow, strongly collimated, and straight for projected distances of tens of kpc from the core before making a sudden transition to diffuse tails or plumes (Figure 1), e.g., [14,22,25,28]. The jet-tail transition is often, but not always, associated with a bright, compact feature (which has been called a warm spot or hot spot). The jet-tail transition occurs over a range of projected distances from a few kpc to ∼80 kpc, e.g., [5,25,28]. In Figure 2, we show the ratio of the length of the jets (from core to hotspot at the jet-tail transition) vs. the average jet length for the WATs in O'Donoghue et al. [5]. We see that the median ratio of jet length is 1.2 and there is no trend for the ratio to change with increasing jet length.
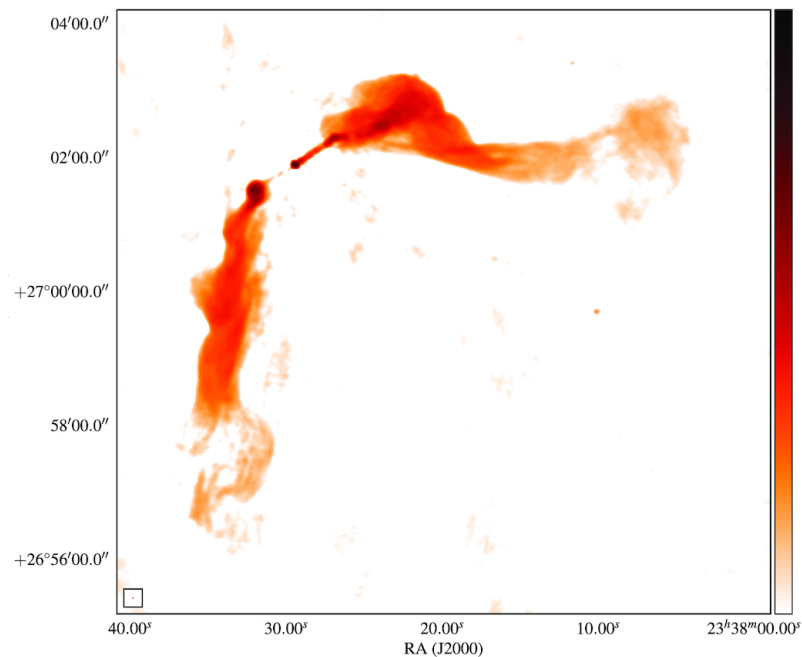
Figure 1. The WAT 3C465 in A2634. JVLA 1.5 GHz image with a resolution of 1.37 × 1.13 arcsec taken from [43].

The bending of the jets occurs either at the jet-tail transition or beyond it, suggesting that the jet-tail transition has made the jet easier to bend. A jet-tail transition is seen in some radio sources associated with Brightest Cluster Galaxies (BCGs) that do not necessarily display the overall large-scale bending of WATs (unless the bending occurs in a plane which is nearly edge-on to our line-of-sight) (e.g., 3C130 [44–46], 0043+201 [25], 0110+152 [25,47], and Hydra A [48]). This implies that the jet-tail transition and the bending are caused by independent mechanisms, as suggested by Hardcastle and Sakelliou [28]. The large-scale bending and the jet-tail transition are discussed further in Section 4.
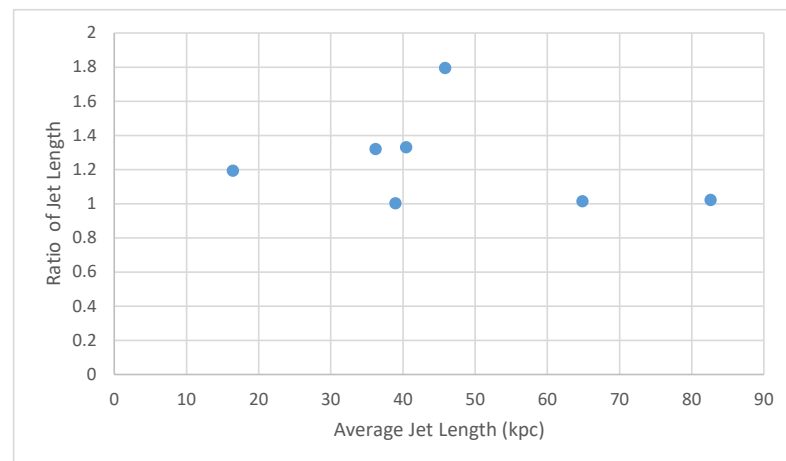

Figure 2. The ratio of jet length (longer/shorter) to average jet length in WATs. Data are taken from O'Donoghue et al. [5].

Caveat Regarding Bending Angle

The bending angle between the tails is sometimes measured and used to either define WATs and/or to search for relationships of other properties with bending angle. However, we note that bending angle is difficult to define and has large systematic errors, especially due to projection effects (see Garon et al. [49] for a discussion). Thus, we recommend against using bending angle. Instead, we suggest using a combination of other properties,

i.e., the jet-tail transition, large-scale bending, and non-parallel tails to indicate that a source is a WAT.

2.3. Jet Velocities

The jet velocities (before the jet-tail transition) have been estimated using the side-to-side ratio of the surface brightness of the two oppositely directed jets on kpc scales [5,28,50]. This analysis assumes the jets are intrinsically uniform and that any differences in surface brightness are due to relativistic Doppler boosting. As there will be intrinsic asymmetry in the jets, these velocity estimates will be an upper limit. In this scenario, the ratio of surface brightness is given by

$$\frac{S_1}{S_2} \simeq \left[\frac{1 - \beta_2 \cos(\theta_2)}{1 - \beta_1 \cos(\theta_1)}\right]^{2-\alpha} \tag{1}$$

where $\beta = v/c$ is the jet velocity which is positive for the approaching (stronger) jet and negative for the receding jet, and θ is the inclination angle of the jet with respect to the line of sight, and α is the jet spectral index, e.g., [51]. The estimates of jet velocity are $\sim$0.2c [5] (11 sources), $\sim$0.3c [28] (7 sources), and $\sim$0.3–0.7c [50] (30 sources[1]), and $\gtrsim$0.5c in 3C465 [43]. Using VLBI to determine jet sidedness in the pc-scale core-jet structures, Venturi et al. [52] estimate jet velocities in the WATs 0836+29 ($v \gtrsim 0.75c$) and 3C465 ($v \gtrsim 0.6c$) and Das et al. [29] find a jet velocity $\sim$0.75c in NGC2329. These relatively high estimated velocities are consistent with the jets not having been disrupted by cool cores (See Section 3.5), although some deceleration is required if the jets were originally ejected with a relativistic velocity.

2.4. Spectral Index Properties

Here, we discuss spectral index properties of WATS, focusing on the most common trends. The largest set of uniform spectral index data is provided by O'Donoghue et al. [25] using VLA observations at 20 and 6 cm. Spectral index data are available for additional individual objects 1919+479 [21,53], NGC2329 (A569) [23,29], NGC 6034 (A2151) [19], 1313+073 [24], 1508+059 (A2029) [26], 3C465 (A2634) [20,43,54,55]. The spectral index of the jets in WATs is relatively flat $\alpha \sim -0.5$ to -0.6 while the tails have a spectral index that tends to steepen with distance down the tail from, e.g., ~ -0.7 to ~ -1.2. The spectral index often does not vary in a linear fashion with distance but can have jumps in value, and regions of relatively constant spectral index.

2.4.1. Evidence for Jet Flow Down the Tails

Spectral aging analyses[2] of the tails of some WATs suggest that there is a problem with particle lifetimes in the tail being too short to account for the surface brightness and spectral index behavior, e.g., [5,20,23,24,43]. This suggests that there is jet flow down the tails, i.e., the tail material does not just sit passively in the ICM. The jet flow can be a source of either fresh particles and/or the energy required to provide particle re-acceleration as apparently needed in the tails of some WATs, e.g., [5,20,23,43,55].

Katz-Stone et al. [27] present a spectral tomography analysis of two WATs previously studied by O'Donoghue et al. [25], 1231+674 and 1433+553. They find two spectral components in the tails; i.e., (1) a central, flatter spectrum, lower polarization "jet", and (2) an outer, steeper-spectrum, higher-polarization "sheath". A similar flatter spectrum ridge is seen in the tails of 3C465 [43]. This is consistent with the presence of jet flow down the tails.

In NGC2329, the inferred projected B field is perpendicular to the tail along the central brightness ridge and parallel to the tail along the edges [23], leading Das et al. [29] to interpret this as a 'spine+sheath" configuration. This is further evidence for jet flow down the tails.

Note that the inferred jet flows do not seem to persist all the way down to the ends of the tails [23,27]. This suggests that the jets dissipate their energy along the way and likely

re-accelerate particles. The deceleration of jet flow in the tails may allow buoyancy (see Section 4.2.2) to dominate at the ends of the tails.

2.5. Polarization Properties

Here, we summarize the polarization properties of WATs, using results from [14,19–29,53,57], again focusing on the general trends. There are only four WATs with estimated Faraday Rotation Measures (RM). The RM is given by

$$RM = 812 \int B_{\parallel} n_e dl \qquad \mathrm{rad\ m^{-2}} \qquad (2)$$

where $B_{\parallel}$ is the magnetic field along the line of sight in milli-gauss, n_e is the electron density in cm^{-3}, and dl is the incremental path length (in pc) along the line of sight. There seems to be real but moderate values (RM < 200 rad m^{-2}) associated with the radio sources, e.g., [20,22,24,53,57].

The RM tends to vary over the source but in a patchy, not a systematic way. Eilek and Owen [57] report that although there are RM structures (RM$\sim$200 rad m^{-2}) which are associated with the radio hotspot in 3C465, the overall RM structure seems more likely to be produced in the ICM of A2634. The only WAT that appears to be in a cool core cluster, 1509+059 (A2029) (Section 3.5), has a much higher RM, up to 4000 rad m^{-2} [26].

The fractional polarization tends to be high in the tails (tens of percent) and increases along the tails (with increasing distance from the core) and also increases from the central brightness ridge to the sides of the tails. The increase in fractional polarization is consistent with the B field becoming more ordered [58,59]. There is some depolarization, i.e., at the same angular resolution, the fractional polarization tends to be higher at higher frequencies. The existence of depolarization combined with the moderate RMs found in some WATs suggests that there is a region of thermal gas and magnetic fields associated with the radio sources.

For optically thin synchrotron emission, the B field direction is perpendicular to the E vector direction. When Faraday Rotation is accounted for, the projected B field direction can be inferred. The inferred projected magnetic field direction is generally parallel to the jets and tails.

3. Host Galaxies and Environments

3.1. Host Galaxies

Early on, it was realized that WATs are typically associated with the dominant galaxy in a cluster of galaxies, e.g., [3,5,25,60–62]. Note that some of the early papers were based on studies of radio sources in clusters, e.g., [3,25,61,62]. However, the association with clusters has held up with more recent studies which include much larger samples and which are unbiased regarding the environment, e.g., [31,63–70], though not all the sources suggested to be WATs in these papers satisfy our classification scheme.

The hosts of WATs are sometimes classified as cD or D galaxies [71], or simply called "dominant". Here, we will refer to these dominant galaxies as BCGs which is consistent with current practice.

Host galaxy properties for the 47 WATs in WATCAT are discussed by Missaglia et al. [31]. We note that WATs tend to have low-excitation emission line nebula which classify them as Low-Excitation Radio Galaxies (LERGs), e.g., [31]. WATs are not always low-excitation, and one of the WATs studied by Missaglia et al. [31] has high-excitation emission lines. De Robertis and Yee [72] reported that 3C465 has weak high-excitation lines with broad Hβ, though this source was later classified as low-excitation [73].

3.2. Environments

WATs are found to be associated with clusters about 50–70% of the time (with some scatter between different studies) [42,66,74,75]. Most of the WATs that are not in clusters are in groups or large-scale filaments, e.g., [49,70,74,76–78]. However, there do seem to be

some WATs in the field, e.g., [49,70,74,79]. The WATs not in clusters are discussed further in Section 3.7.

Although WATs are found preferentially in clusters, not all clusters have WATs. Only about 6% of clusters have WATs [74]. This is likely because powerful radio sources are rare, and the bending of the radio source requires certain conditions.

3.3. Relative Velocities of WAT Hosts

Since WAT hosts in clusters are typically BCGs, they were initially expected to move slowly with respect to the ICM, e.g., [3,14,80]. This expectation was based on early radial velocity measurements of BCGs and their clusters which suggested that BCGs move very slowly in the cluster gravitational potential ($\sim$100 km s^{-1}), e.g., [81]. This expectation was also a consequence of the idea that equipartition of kinetic energy among cluster galaxies in relaxed clusters would result in the more massive galaxies moving more slowly, and the most massive galaxy being nearly at rest at the centre of the cluster gravitational potential, e.g., [3,82,83]. However, this led to problems with understanding how the tails in WATs are bent due to the low ram pressure expected in this scenario, e.g., [4,14,80].

Note that it is important to determine velocities of BCGs independent of their radio properties. This is because selecting WATs might preferentially select BCGs with most of their peculiar velocity in the plane of the sky.

Subsequent studies of radial velocities of cluster galaxies showed that there was a significant population of BCGs which have large ($\sim$200–400 km s^{-1}) radial velocities with respect to their clusters, e.g., [84–89]. In addition, BCGs are sometimes not located at the cluster centre, although they are located in local peaks in galaxy density, e.g., [90–92]. The BCGs with spatial and/or velocity offsets are found in clusters with significant substructure consistent with these clusters still growing via mergers of clusters and/or subclusters, e.g., [87,89,93]. About 30–70% (so likely the majority) of rich clusters show substructure in the distribution of either gas or galaxies, e.g., [94,95].

3.4. Are WATs Preferentially Found in Merging Clusters?

Given that BCGs can have significant velocities in merging clusters, what is the evidence that WATs are found in merging clusters? X-ray studies of the cluster environments of numerous individual WATs show elongated and/or clumpy X-ray emitting gas, with the radio tails oriented in the direction of the X-ray elongation (see Figure 3), e.g., [10,96–109] and/or bow shocks and cold fronts, e.g., [110–115]. None of the existing X-ray analyses find that WATs are in regular, relaxed clusters except possibly in A2029 [116], although the detection of sloshing gas suggests a recent merger in this cluster as well [110].

In addition, galaxy radial velocities reveal merging clusters in some systems, e.g., [76,99,100,109,117–119]. As a counterexample, Wing and Blanton [75] do not find a significant difference in the amount of optical substructure in clusters with WATs vs. other kinds of radio sources. However, it is likely that the details of the bulk motions of the ICM (Section 3.4.1) matter more than just the presence of substructure. To summarize, there is clear evidence that WATs are found in clusters which are in the process of merging.

3.4.1. Sloshing Gas in Merging Clusters

One important consequence of cluster mergers is that they can generate large-scale ($\sim$100 kpc), long-lived ($\sim$1 Gyr) motions of the ICM, called sloshing (for a review, see Markevitch and Vikhlinin [120]). The presence of sloshing gas can be inferred using observations of shocks and cold fronts in the ICM, e.g., [95,120]. Numerical simulations of cluster mergers predict gas velocities of up to $\sim$1000 km s^{-1}, e.g., [121–124], which is consistent with estimates obtained from analysis of cold fronts and shocks, e.g., [120].
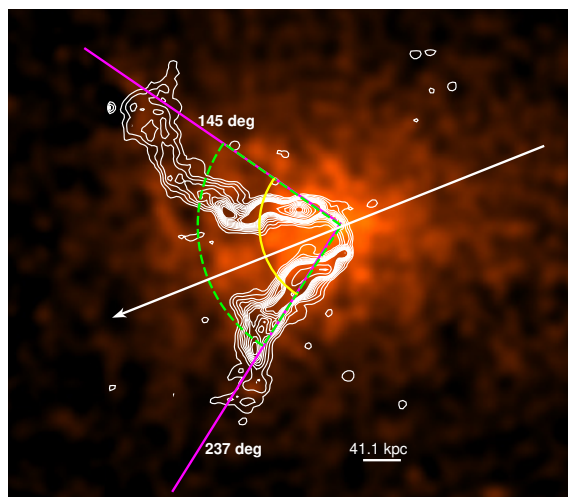
Figure 3. The WAT 1233+168 in the merging cluster A1569. Contours of the VLA image are shown on the Chandra X-ray image. The arrow shows the bisection of the angle between the two tails of the WAT, showing that the elongated X-ray emission extends down the middle of the radio tails. The Figure, including all annotations, is from Tiwari and Singh [115].

Sloshing gas has been inferred in several clusters with WATs, including A98 [111,114], A1569 (see Figure 3) [100,115], A1763 [113], A2029 [110], and RXJ0334.2-0111 [112]. Since sloshing is expected to be common in cluster mergers, e.g., [120] and nearly all WATs in clusters appear to be in merging clusters (Section 3.4), we expect sloshing to provide significant ram pressure which should be accounted for in models for WATs (to be discussed in Section 4.2.4).

3.5. Why Do WATs Avoid Clusters with Cool Cores?

So far, studies of the X-ray properties of clusters containing WATs indicate that WATs are not found in clusters with cool cores (previously known as cooling flows), e.g., [5,10,98,99,107,125,126] (although there are a few counter-examples where the cool cores have not yet been destroyed by a merger [108,116]). Why does this matter?

1. X-ray studies show that cool cores are apparently disrupted by cluster mergers, e.g., [127–129]. There is support for this from recent numerical simulations, e.g., [130–132]. Since WATs are in clusters undergoing mergers (Section 3.4), WATs should not be in clusters with cool cores if cool cores are disrupted by the type of cluster mergers that create WATs;
2. Radio jets may be disrupted in cool cores. Soker and Sarazin [133] suggested that cool cores could disrupt radio jets on sub-kpc scales. This is consistent with the amorphous radio morphology often seen in cool cores, e.g., [125,134–136]. In addition, VLBI shows two-sided jets on the pc scale in some cool core radio sources, e.g., [137,138], suggesting that the initially relativistic jets have already decelerated to sub-relativistic speeds on pc scales. However, WATs have narrow, relatively straight, powerful jets out to tens of kpc from the nucleus with estimated jet velocities of 0.2–0.7c (Section 2), consistent with the jets in WATs not being disrupted on sub-kpc scales by a cool core.

3.6. Using WATs to Find Clusters of Galaxies

It is clear that WATs are preferentially found in clusters of galaxies, although we now appreciate that these clusters generally appear to be merging clusters (Section 3.4) without cool cores (Section 3.5). Hintzen and Scott [6] were apparently the first to suggest that WATs could be used to find clusters of galaxies. They tested this by obtaining Very Large Array (VLA) observations of radio-loud quasars and then obtaining optical images of the fields [7,139]. Hintzen [7] reported that the fields of the quasars with WATs had three times the number of excess galaxies as quasars with undistorted radio structure,

thus confirming the suggestion that WATs could be used to find clusters. Sixteen years later, work began in earnest to apply this technique starting with Blanton et al. [8]. There have now been many studies which have successfully used WATs to find and/or study clusters, e.g., [8,9,49,63,64,69,74,77,79,140–150]. In the COBRA survey [141], the distribution of redshifts of clusters found using WATs peaks around $z \sim 1$ and extends out to $z \simeq 3$ [149]. So far, WATs have been used to infer the dynamical state of a cluster, e.g., [9,145] as well as the gas density in groups, e.g., [143,151] and in a filament [77]. Large samples (a few hundreds to thousands) of WATs have been found in current radio surveys, e.g., FIRST/VLA [32,49,63], LotSS/LOFAR [42,68], and TIFR/GMRT [152]. Note that the lower-resolution surveys will not generally resolve the jet-tail transition; however, the overall bending of the source into non-parallel tails can be seen and used to classify the radio morphology as WAT, e.g., [31,68,152]. Dehghan et al. [153] point out that the EMU/ASKAP survey [154] is expected to detect around 440,000 WATs. This will open up a new regime in the search for clusters and determination of their properties, e.g., [155].

3.7. What about WATs Outside of Clusters?

It is clear the WATs are preferentially found in merging clusters. What are the environments of WATs which are not in clusters (i.e., groups, filaments, and the field)? The studies cited below use different methods for identifying WATs and characterizing their environments, and often group WATs and NATs together as bent radio sources, but there is some consensus.

Wing and Blanton [63] determine the richness of the environments of bent double radio sources chosen from FIRST. About 80% of the bent doubles are WATs (Blanton, private communication). Using SDSS images they count the galaxies brighter than $M_r = -19$ within 1.0 Mpc of the bent radio source correcting for background galaxies, $N_{1.0}^{-19}$. A radius of 1.0 Mpc was chosen to optimize detection of clusters. They find that about 63% of the bent FRI sources are in rich clusters, 17% in poor clusters, about 10% in groups, and another 10% in sparser environments.

Liu et al. [67] determine galaxy richness using the parameter $N_{0.5}^{-19}$ for a sample of C-shaped sources taken from the classifications of FIRST sources by Proctor [156]. The C-shaped sources include both WATs and NATs. They note that 52% of the C-shaped sources are identified with BCGs, consistent with them being WATs, but they do not give separate clustering statistics for WATs and NATs. Liu et al. [67] find that 83% of the C-shaped sources are in a rich environment (defined to be $N_{0.5}^{-19} \gtrsim 10$).

Mingo et al. [42] report 195 WATs found in the LoTSS survey. The find that 48% of the WATs are associated with clusters in the LoTSS environmental catalog [157] consisting of clusters derived from SDSS data. The remaining 52% of WATs would be in groups or in the field, i.e., in systems with halo mass $M_{500} < 10^{14}$ $M_\odot$.

Pal and Kumari [68] present a list of 45 additional WATs found in the LoTSS survey (supplemental to Mingo et al. [42]). They report that 25/45 (55%) are associated with known clusters found via a search with NED. Since the list of clusters found in NED is likely to be incomplete this leaves < 45% of WATs in groups and the field.

Bhukta et al. [152] present a list of 203 WATs found in the TIFR/GMRT survey. They find that 89/203 (44%) of the WATs are identified with known clusters leaving < 66% in groups and the field.

Morris et al. [70] examine a sample of 185 bent doubles chosen by visual confirmation of FIRST sources classified automatically [158]. Morris et al. [70] estimate that 75% of their bent doubles are actually WATs. They parameterize the local environments via a friends-of-friends approach using data from DECaLS and unWISE. They find that 17% of their bent doubles are associated with isolated or paired galaxies, 62% are the brightest galaxy in a group, and 21% are in a group but are not the brightest galaxy. These results are consistent with those of Garon et al. [49] who find that bent radio sources outside of clusters are still found in regions of significant galaxy overdensity (i.e., are in groups).

Thus, there is consensus that there are significant numbers of WATs outside of clusters, and most of those are in groups. The environments of WATs which are not in clusters should be investigated. Where possible, studies should make it clear which of their bent double sources are WATs.

It seems likely that ram pressure does bend the jets in WATs (see Section 4.2.4). Thus, WATs can be used to probe densities and velocities outside of clusters. As mentioned above, WATs have been used to estimate the gas density in groups, e.g., [143,151] and in a filament [77].

4. Models for WATs

Here, we discuss models which attempt to explain the two main features of WATs—(1) the sudden jet-tail transition and (2) the overall bending of WATs.

4.1. What Causes the Jet-Tail Transition?

The origin of the jet-tail transition is a well-known and interesting problem, e.g., [4,5,14,28,47,103,159,160]. Hardcastle and Sakelliou [28] suggest that the jet-tail transition is independent from the problem of bending the tails due to (1) the existence of sources with a jet-tail transition which do not show overall bending (3C130 [44–46], 0043+201 [25], 0110+152 [25,47], and Hydra A [48]), and (2) the fact that a few WATs show bending that occurs before the jet-tail transition (0647+693 [28,161], CWAT-01 [9], and 1919+479 [21,53,80]). We also note that the jets in NATs are bent independent of a jet-tail transition, though the bending in NATs is much more gradual than in WATs, e.g., [18,162]. The nature of the jet-tail transition seems complex because some jets show a hot spot at the transition, and others do not. In addition, in some WATs, the jets seem to continue for some distance down the tails after the transition (e.g., 1231+674 [27,28], 1433+553 [27], and NGC2329 [23,29]). Nevertheless, in nearly all cases, the jets are bent either at the jet-tail transition or beyond it, suggesting that the transition makes the jets easier to bend.

The jet disruption occurs after the jet has propagated for several tens of kpc, e.g., [25,28]. This distance is near the expected transition between the host BCG ISM and the ICM [24,47,103,160]. At this point, it is not clear what happens at the ISM/ICM transition to disrupt the jet. Suggestions include (1) the development of instabilities in the jet (either current-driven or Kelvin–Helmholtz) [22,103,159], (2) the transition from a high-density ISM to lower-density ICM [103,159], (3) the transition from a cool BCG ISM to hotter ICM [47], (4) passage through a sharp pressure drop [4], (5) and passage though a shock [103,163,164]. Here, we discuss these hypotheses in more detail.

4.1.1. Current-Driven Instabilities

It is possible that instabilities play a role in the jet-tail transition. In particular, current-driven instabilities (CDI) can be important in jets with a dominant magnetic field, e.g., [165–168]. Here, we briefly discuss CDI and in the section below, we discuss Kelvin–Helmholtz instabilities. Recent magnetohydrodynamical (MHD) simulations of jets show that CDI can disrupt the jets for a certain range of ambient density profile, jet magnetization, magnetic field topology, and jet power [39,167,169–171]. In addition, two MHD simulations have specifically addressed WAT sources (moderate power, magnetized jets in a cross-wind) [167,172]. The simulation by Massaglia et al. [167] is fairly successful in producing WAT morphology, including jet disruption with warm spots and subsequent bent tails. We regard this work as very promising.

4.1.2. Kelvin–Helmholtz Instabilities

Kelvin–Helmholtz instabilities are thought to influence jet morphology and may result in jet disruption, e.g., [173–176]. These instabilities have been suggested as a mechanism for jet-tail transition [103,159]. However, there are two problems with this hypothesis. The two jets make the jet-tail transition at about the same distance from the galaxy nucleus which would demand almost identical growth of the instability on both sides of the galaxy.

Additionally, the jets seem to remain narrow and straight until the transition, i.e., they do not seem to show a growing instability.

Hardcastle and Sakelliou [28] show that the projected length of the jet before the jet-tail transition is larger in clusters with lower X-ray temperature. This is evidence that a property of the ICM is related to the jet-tail transition. In addition, in four sources, the jet-tail transition appears to occur at the sharp gradient in the gas temperature as the cooler ISM of the BCG transitions to the hotter ICM [47,103,160]. Thus, we next consider hypotheses that are related to the ISM/ICM transition.

4.1.3. A Transition from High-Density, Cool ISM to Lower-Density, Hotter ICM

Another possibility is that the jet disrupts when it transitions from the high-density, cooler ISM of the host BCG to the lower-density, hotter ICM [47,103,159] or through a sharp pressure drop [4]. Note that the jets in many non-WAT radio galaxies survive the transition from a host galaxy ISM to IGM, so there must be something special about the transition from a BCG ISM to a cluster ICM that causes the jet-tail transition. The analytical modelling [177] and numerical simulations [178,179] suggest that crossing the ISM/ICM interface can affect the properties of jets, although the results are model-dependent. Under some assumptions, low-Mach-number jets may flare and decelerate upon crossing the ISM/ICM interface [177,178].

Hardee et al. [180] carry out numerical simulations which suggest that jets which propagate in atmospheric gradients can suppress backflow, causing the jets to interact directly with the ambient medium. This can lead to rapid disruption of the jet. An alternative way to remove the protective cocoon from the jet is "cocoon crushing" [28,46]. In this scenario, the pressure in the cocoon drops with time so that the cocoon becomes underpressured with respect to the ambient medium. The cocoon is then crushed by the ambient medium and is driven outwards by buoyancy forces. We suggest that state-of-the-art simulations are needed to probe the behaviour of jets as they propagate from a BCG ISM to the ICM.

4.1.4. Shocks at the ISM/ICM Interface

Norman et al. [163] suggest that a planar shock at the ISM/ICM interface could disrupt a jet. Loken et al. [164] support this hypothesis and suggest that either a planar or an oblique shock (with a shock Mach number greater than the jet Mach number) can disrupt the jet. Shocks could arise if the jet transitions the ISM/ICM interface at an angle to the normal [178] or if there is a bow shock due to the motion of the ICM relative to the host galaxy [103]. Current X-ray observations have not revealed any features at the ISM/ICM interface which could account for the jet-tail transition [47,160]. However, deeper observations are required for a definitive test.

4.1.5. Summary of Section 4.1

The hypotheses which invoke "something happening" at the ISM/ICM interface to disrupt the jet are not ruled out by the current observational constraints. In general, a deeper understanding of the gas properties at the ISM/ICM boundary is required in order to understand the disruption of the jets. The MHD simulations by Massaglia et al. [167] also show promise. Additional, high-resolution MHD simulations are needed to probe the behaviour of jets as they cross the ISM/ICM interface.

4.2. What Bends WATs?

As discussed in Section 3, in the 1980s, it was thought that there was insufficient ram pressure to bend the jets in WATs. This led to a number of alternate hypotheses [14]. Here, we discuss a few of the alternate hypotheses before returning to ram pressure.

4.2.1. Collisions with Dense Clouds

Eilek et al. [14] suggested collisions of the jets with dense clouds could bend the jets in 3C465. Jet–cloud collisions were also invoked for 1919+479 [53]. Numerical simulations of jet–cloud collisions suggest that jets can be disrupted and deflected under certain conditions, e.g., [181–183]. However, there are problems with this hypothesis. The dense clouds have to placed so that the two jets are bent at about the same distance from the nucleus and are bent in roughly the same direction. This seems fortuitous. The origin of the clouds is problematic. If WATs were in cool core clusters, then we might expect clouds to be condensing from the ICM, but we know that WATs avoid cool core clusters (Section 3.5). In addition, there is no observational evidence for the population of clouds that would be required around WATs, e.g., [184]. Thus, it seems unlikely that jet–cloud collisions bend the jets in WATs, although there is evidence for jet–cloud collisions in other types of radio sources, e.g., [185].

4.2.2. Buoyancy

Buoyant forces may shape the diffuse, low-density parts of radio galaxies [186–188]. Eilek et al. [14] ruled out buoyancy as the mechanism for the sudden bending of the jets in 3C465. However, it is possible that buoyancy is responsible for more gradual bending of the tails seen in some WATs, e.g., [21,80,96,102]. Estimates of electron densities in the tails based on polarimetry[3] suggest they are less dense than the ambient ICM, e.g., [21,24,53,80]. Estimates of densities from constraints on the bending of the jets are also consistent with densities less than that of the ICM, e.g., [5,10,14,160]. Thus, in principle, the tails of WATs should be subject to buoyant forces in the ICM.

The observational evidence for buoyancy comes from studies of the spatial relationship between the radio source and the hot ICM as traced by its X-ray emission. The curvature in the tails could be caused by buoyancy in 4C34.16 [102], 3C465 [103], 0647+693 [10], and 1233+168 [115]. Thus, we expect the tails to be buoyant and there are indeed a few examples of sources which show gradual curvature consistent with buoyancy. Note that projection effects complicate the interpretation of the radio and X-ray morphology. It is possible that the large-scale curvature of the tails could be due to some other mechanism, e.g., complex motions in the sloshing gas.

4.2.3. Electrodynamic Effects ($j \times B$)

Eilek et al. [14] suggested that if the jet carries a current and there is an organized magnetic field in the cluster, then the Lorentz force ($j_z \times B_{\rm ICM}$, where j_z is the axial current in the jet and $B_{\rm ICM}$ is the magnetic field in the ICM) might bend the jets. Observations of cluster RMs and cluster radio haloes confirm that there is a magnetic field of strength ~ 1 μG in the ICM, e.g., [1]. There are theoretical arguments for a current in radio jets, e.g., [190–193]. Furthermore, observational evidence for helical magnetic fields in jets supports the existence of currents in jets, e.g., [194]. Thus, it seems plausible that the Lorentz force may influence the behaviour of jets.

From Ampere's law, the axial current in the jet is

$$j_{\rm z} = 1.5 \times 10^{13} \left(\frac{B_\phi}{\mu{\rm G}} \right) \left(\frac{r_j}{\rm kpc} \right) \qquad \text{Amperes} \qquad (3)$$

where B_ϕ is the azimuthal field at the surface of the jet and r_j is the radius of the jet[4]. Eilek et al. [14] adopt a value for B_ϕ of the equipartition value (essentially assuming that the axial current produces all of the jet magnetic field) and find that an ambient field $B_{\rm ICM} \sim 1$μG is required to bend the jets. This is a plausible value. However, Eilek et al. [14] note two problems with the Lorentz force in the case of 3C465. (1) The external B field responsible for bending the jets must be located at the two hot spots where the jets bend, and (2) the Lorentz force must bend the jets to the same side of the jet ejection axis. Further, the turbulent ICM in a merging cluster may disorder the magnetic field.[5] These

conditions make it unlikely that the Lorentz force bends the jets in WATs, but applications in other types of jets cannot be currently ruled out. In particular, Fendt and Zinnecker [195] suggest that the Lorentz force might bend protostellar jets.

4.2.4. Ram Pressure Due to Cluster Mergers

We have shown above that WATs are preferentially found in merging clusters (Section 3.4) where there is expected to be large-scale bulk motion ($v \gtrsim 1000$ km s^{-1}) of the ICM (sloshing, Section 3.4.1). It has been suggested that large-scale sloshing provides sufficient ram pressure to bend the jets in WATs, e.g., [76,97,99,100,104,121,196].

Several numerical simulations have shown that jets propagating in such clusters can be disrupted and bent, forming structures somewhat similar to those seen in WATs, e.g., [164,172,197] but not matching in the details.

What do the analytical calculations indicate? Since the jets in WATs are not relativistic (Section 2.3), we can use the non-relativistic version of Euler's equation [198] for ram pressure bending

$$\frac{\rho_j v_j^2}{R} = \frac{\rho_{ICM} \Delta v^2}{r_j} \tag{4}$$

where ρ_j and ρ_{ICM} are the densities in the jet and the ICM, respectively, Δv is the relative velocity of the jet and the ICM (due to some combination of host BCG motion and bulk flows in the ICM), R is the radius of curvature of the bending, and r_j is the radius of the jet, e.g., [12–15]. We note that R and r_j are estimated from radio images, ρ_{ICM} is estimated from X-ray observations, Δv is uncertain, and ρ_j and v_j are highly uncertain. Some authors have put estimates for these parameters in Equation (4) and concluded that the jets can be bent by ram pressure [24,119,199]. Some authors have adopted additional constraints on the jet properties. Eilek et al. [14] assume that the radio luminosity of the tails in 3C465 is powered by the jets

$$L_{rad} \simeq \epsilon \pi r_j^2 \rho_j v_j^3 / 2 \tag{5}$$

for a non-relativistic jet, where ϵ is the efficiency of conversion of jet kinetic energy flux to luminosity. This approach was used in estimating constraints on the jets in NATs [12,15]. This assumption has been considered for WATs [5,100,160] and the jets that satisfy the requirements of Equations (4) and (5) tend to be low-density and fast. Several studies find that ram pressure from large-scale bulk motions ($\Delta v \gtrsim 1000$ km s^{-1}) can bend the jets in WATs [9,10,100,107,112,160].[6] Thus, at this point, we suggest that ram pressure bending in clusters with significant bulk motion of the ICM is the most likely mechanism for bending WATs.

4.2.5. What about WATs That Are Not in Clusters of Galaxies?

WATs are found both in and out of clusters (Section 3.7). The fact that some WATs are not in clusters is somewhat puzzling given the need for ram pressure. However, rather than invoke a separate bending mechanism for non-cluster WATs, we suggest that there is a source of ram pressure in these environments which is capable of bending the WATs. This should be tested by detailed studies of non-cluster WATs [16].

5. Summary

We review the properties of Wide-Angle-Tail (WAT) radio sources. The WAT radio sources are powerful, bent radio sources that are typically associated with a dominant galaxy in a cluster or group of galaxies. For the purposes of this review, the radio morphology properties that define WATs are (1) a sudden jet-tail transition on scales of tens of kpc from the core, (2) overall bending of the tails to one side, and (3) non-parallel tails.

WATs exhibit a narrow range of radio luminosity. Consistent with the FRI/FRII paradigm, we suggest that there is a minimum radio luminosity required to produce the straight, well-collimated jets that extend to several tens of kpc from the core. Further,

we suggest there is a maximum radio luminosity required to allow the jet disruption mechanism to cause the jet-tail transition.

Estimates of the density in the tails from polarimetry and bending arguments suggest the tails are less dense than the ICM and should be buoyant. There are a few examples of WATs with gradual curvature in the tails which might be due to buoyancy.

There are ridges in intensity and flatter spectral indexes along the tails suggesting there is jet flow down the tails for at least some of their length. The short estimated electron radiative lifetimes require particle re-acceleration in the tails. Under the assumption that relativistic effects dominate the jet appearance, jet sidedness ratios give estimates of jet velocity of ∼0.2–0.7c on kpc scales. The mechanism for the rapid jet-tail transition is still uncertain but it seems to occur near the transition from the host ISM to ICM. MHD simulations suggest current-driven instabilities may be involved, although more simulations are needed. The jet-tail transition appears to make the jets easier to bend.

WATs are typically hosted by brightest cluster galaxies in clusters which are currently merging and do not contain cool cores. Thus, WATs can be used as tracers of merging clusters. The merging also produces large-scale bulk motions in the ICM which can provide sufficient ram pressure to bend the jets. We suggest that although the Lorentz force may not bend the jets in WATs, it may be relevant in other sources, e.g., protostellar jets.

Author Contributions: Both authors contributed to the writing of the article. All authors have read and agreed to the published version of the manuscript.

Data Availability Statement: Not applicable.

Conflicts of Interest: The authors declare no conflict of interest.

Abbreviations

The following abbreviations are used in this manuscript:

AGN	Active Galactic Nuclei
BCG	Brightest Cluster Galaxy
CDI	Current-driven instability
HT	Head-Tail
ICM	Intracluster Medium
IGM	Intergalactic Medium
ISM	Interstellar Medium
LERG	Low-Excitation Radio Galaxy
MHD	Magnetohydrodynamical
NAT	Narrow Angle Tail
VLA	Very Large Array
VLBI	Very Long Baseline Interferometry
WAT	Wide-Angle-Tail

Notes

[1] There is some overlap between the samples studied by O'Donoghue et al. [5], Hardcastle and Sakelliou [28], Jetha et al. [50]

[2] Young et al. [56] note that the simple electron aging models are not a good fit to the spectral index data of two WATs, 1231+674 and 1433+553. This could be due to complexity in the magnetic field structure and electron populations.

[3] Estimates of internal electron densities from polarimetry are complicated, e.g., [59,189].

[4] The SI unit for current seemed more appropriate here.

[5] This was suggested to us by one of our referees.

[6] An additional assumption that is occasionally adopted is that ram pressure will balance buoyancy forces at some point in the tails [102,103]. However, this assumes constant jet velocity down the tails which may not be valid (See Section 2.4.1).

References

1. Feretti, L.; Giovannini, G. Clusters of Galaxies in the Radio: Relativistic Plasma and ICM/Radio Galaxy Interaction Processes. In *A Pan-Chromatic View of Clusters of Galaxies and the Large-Scale Structure*; Plionis, M., López-Cruz, O., Hughes, D., Eds.; Springer: Dordrecht, The Netherlands 2008; Volume 740, pp. 143–176. [CrossRef]
2. Saikia, D.J. Jets in radio galaxies and quasars: An observational perspective. *J. Astrophys. Astron.* **2022**, *43*, 97–127. [CrossRef]
3. Owen, F.N.; Rudnick, L. Radio sources with wide-angle tails in Abell clusters of galaxies. *Astrophys. J.* **1976**, *205*, L1–L4. [CrossRef]
4. Burns, J.O. Wide-angle tailed radio galaxies. *Can. J. Phys.* **1986**, *64*, 373–377. [CrossRef]
5. O'Donoghue, A.A.; Eilek, J.A.; Owen, F.N. Flow Dynamics and Bending of Wide-Angle Tailed Radio Sources. *Astrophys. J.* **1993**, *408*, 428–445. [CrossRef]
6. Hintzen, P.; Scott, J.S. The use of radio source morphology in detecting clusters of galaxies associated with QSOs. *Astrophys. J.* **1978**, *224*, L47–L50. [CrossRef]
7. Hintzen, P. Wide-angle radio tail QSOs as members of clusters of galaxies. II. Direct optical observations and spectroscopy of QSO fields. *Astrophys. J. Suppl. Ser.* **1984**, *55*, 533–550. [CrossRef]
8. Blanton, E.L.; Gregg, M.D.; Helfand, D.J.; Becker, R.H.; White, R.L. FIRST Bent-Double Radio Sources: Tracers of High-Redshift Clusters. *Astrophys. J.* **2000**, *531*, 118–136. [CrossRef]
9. Smolčić, V.; Schinnerer, E.; Finoguenov, A.; Sakelliou, I.; Carilli, C.L.; Botzler, C.S.; Brusa, M.; Scoville, N.; Ajiki, M.; Capak, P.; et al. A Wide-Angle Tail Radio Galaxy in the COSMOS Field: Evidence for Cluster Formation. *Astrophys. J. Suppl. Ser.* **2007**, *172*, 295–313. [CrossRef]
10. Douglass, E.M.; Blanton, E.L.; Clarke, T.E.; Randall, S.W.; Wing, J.D. The Merger Environment of the Wide Angle Tail Hosting Cluster A562. *Astrophys. J.* **2011**, *743*, 199–211. [CrossRef]
11. Jones, T.W.; Nolting, C.; O'Neill, B.J.; Mendygral, P.J. Using collisions of AGN outflows with ICM shocks as dynamical probes. *Phys. Plasmas* **2017**, *24*, 041402. [CrossRef]
12. Jones, T.W.; Owen, F.N. Hot gas in elliptical galaxies and the formation of head-tail radio sources. *Astrophys. J.* **1979**, *234*, 818–824. [CrossRef]
13. Begelman, M.C.; Rees, M.J.; Blandford, R.D. A twin-jet model for radio trails. *Nature* **1979**, *279*, 770–773. [CrossRef]
14. Eilek, J.A.; Burns, J.O.; O'Dea, C.P.; Owen, F.N. What bends 3C 465 ? *Astrophys. J.* **1984**, *278*, 37–50. [CrossRef]
15. O'Dea, C.P. Constraints on bent beams in narrow angle tail radio sources. *Astrophys. J.* **1985**, *295*, 80–88. [CrossRef]
16. Morsony, B.J.; Miller, J.J.; Heinz, S.; Freeland, E.; Wilcots, E.; Brüggen, M.; Ruszkowski, M. Simulations of bent-double radio sources in galaxy groups. *Mon. Not. R. Astron. Soc.* **2013**, *431*, 781–792. [CrossRef]
17. Rudnick, L.; Owen, F.N. Head-tail radio sources in clusters of galaxies. *Astrophys. J.* **1976**, *203*, L107–L111. [CrossRef]
18. O'Dea, C.P.; Owen, F.N. The global properties of a representative sample of 51 narrow-angle-tail radio sources in the directions of Abell clusters. *Astron. J.* **1985**, *90*, 954–972. [CrossRef]
19. Valentijn, E.A.; Perola, G.C. A Westerbork survey of rich clusters of galaxies. V. Multi-frequency observations of the radio tail galaxy NGC 6034 in the Hercules cluster. *Astron. Astrophys.* **1978**, *63*, 29–35.
20. van Breugel, W.J.M. Multifrequency observations of extended radio galaxies III: 3C 465. *Astron. Astrophys.* **1980**, *88*, 248–258.
21. Robertson, J.G. Multifrequency observations of the complex radio galaxy 1919+479 (4C 47.51). *Astron. Astrophys.* **1984**, *138*, 41–48.
22. Leahy, J.P. 3C 465 : Dynamics of a wide-tail radio source. *Mon. Not. R. Astron. Soc.* **1984**, *208*, 323–345. [CrossRef]
23. Feretti, L.; Giovannini, G.; Gregorini, L.; Padrielli, L.; Roland, J.; Valentijn, E.A. The wide angle tailed radio source NGC 2329 in the cluster A 569. *Astron. Astrophys.* **1985**, *147*, 321–327.
24. Patnaik, A.R.; Malkan, M.A.; Salter, C.J. Multifrequency observations of the wide-angle tail radio source 1313+073. *Mon. Not. R. Astron. Soc.* **1986**, *220*, 351–362. [CrossRef]
25. O'Donoghue, A.A.; Owen, F.N.; Eilek, J.A. VLA Observations of Wide-Angle Tailed Radio Sources. *Astrophys. J. Suppl. Ser.* **1990**, *72*, 75–131. [CrossRef]
26. Taylor, G.B.; Barton, E.J.; Ge, J. Searching for Cluster Magnetic Fields in the Cooling Flows of 0745-191, A2029, and A4059. *Astron. J.* **1994**, *107*, 1942–1952. [CrossRef]
27. Katz-Stone, D.M.; Rudnick, L.; Butenhoff, C.; O'Donoghue, A.A. Coaxial Jets and Sheaths in Wide-Angle-tailed Radio Galaxies. *Astrophys. J.* **1999**, *516*, 716–728. [CrossRef]
28. Hardcastle, M.J.; Sakelliou, I. Jet termination in wide-angle tail radio sources. *Mon. Not. R. Astron. Soc.* **2004**, *349*, 560–575. [CrossRef]
29. Das, S.; Kharb, P.; Morganti, R.; Nandi, S. The peculiar WAT NGC 2329 with Seyfert/FR I-like radio lobes. *Mon. Not. R. Astron. Soc.* **2021**, *504*, 4416–4427. [CrossRef]
30. Reynolds, J.E. Projection Effects and Radio Source Morphology. *Publ. Astron. Soc. Aust.* **1980**, *4*, 74–76. [CrossRef]
31. Missaglia, V.; Massaro, F.; Capetti, A.; Paolillo, M.; Kraft, R.P.; Baldi, R.D.; Paggi, A. WATCAT: A tale of wide-angle tailed radio galaxies. *Astron. Astrophys.* **2019**, *626*, A8–27. [CrossRef]
32. Sasmal, T.K.; Bera, S.; Pal, S.; Mondal, S. A New Catalog of Head-Tail Radio Galaxies from the VLA FIRST Survey. *Astrophys. J. Suppl. Ser.* **2022**, *259*, 31–40. [CrossRef]
33. Fanaroff, B.L.; Riley, J.M. The morphology of extragalactic radio sources of high and low luminosity. *Mon. Not. R. Astron. Soc.* **1974**, *167*, 31P–36P. [CrossRef]
34. Bridle, A.H.; Perley, R.A. Extragalactic Radio Jets. *Annu. Rev. Astron. Astrophys.* **1984**, *22*, 319–358. [CrossRef]

35. Baum, S.A.; Zirbel, E.L.; O'Dea, C.P. Toward Understanding the Fanaroff-Riley Dichotomy in Radio Source Morphology and Power. *Astrophys. J.* **1995**, *451*, 88–99. [CrossRef]

36. Bicknell, G.V. Relativistic Jets and the Fanaroff-Riley Classification of Radio Galaxies. *Astrophys. J. Suppl. Ser.* **1995**, *101*, 29–39. [CrossRef]

37. Kaiser, C.R.; Best, P.N. Luminosity function, sizes and FR dichotomy of radio-loud AGN. *Mon. Not. R. Astron. Soc.* **2007**, *381*, 1548–1560. [CrossRef]

38. Laing, R.A.; Bridle, A.H. Systematic properties of decelerating relativistic jets in low-luminosity radio galaxies. *Mon. Not. R. Astron. Soc.* **2014**, *437*, 3405–3441. [CrossRef]

39. Tchekhovskoy, A.; Bromberg, O. Three-dimensional relativistic MHD simulations of active galactic nuclei jets: Magnetic kink instability and Fanaroff-Riley dichotomy. *Mon. Not. R. Astron. Soc.* **2016**, *461*, L46–L50. [CrossRef]

40. Massaglia, S.; Bodo, G.; Rossi, P.; Capetti, S.; Mignone, A. Making Faranoff-Riley I radio sources. I. Numerical hydrodynamic 3D simulations of low-power jets. *Astron. Astrophys.* **2016**, *596*, A12. [CrossRef]

41. Ehlert, K.; Weinberger, R.; Pfrommer, C.; Pakmor, R.; Springel, V. Simulations of the dynamics of magnetized jets and cosmic rays in galaxy clusters. *Mon. Not. R. Astron. Soc.* **2018**, *481*, 2878–2900. [CrossRef]

42. Mingo, B.; Croston, J.H.; Hardcastle, M.J.; Best, P.N.; Duncan, K.J.; Morganti, R.; Rottgering, H.J.A.; Sabater, J.; Shimwell, T.W.; Williams, W.L.; et al. Revisiting the Fanaroff-Riley dichotomy and radio-galaxy morphology with the LOFAR Two-Metre Sky Survey (LoTSS). *Mon. Not. R. Astron. Soc.* **2019**, *488*, 2701–2721. [CrossRef]

43. Bempong-Manful, E.; Hardcastle, M.J.; Birkinshaw, M.; Laing, R.A.; Leahy, J.P.; Worrall, D.M. A high-resolution view of the jets in 3C 465. *Mon. Not. R. Astron. Soc.* **2020**, *496*, 676–688. [CrossRef]

44. Jaegers, W.J. The cluster around 3C130. *Astron. Astrophys.* **1983**, *125*, 172–174.

45. Hardcastle, M.J. Jets, plumes and hotspots in the wide-angle tail source 3C 130. *Mon. Not. R. Astron. Soc.* **1998**, *298*, 569–576. [CrossRef]

46. Hardcastle, M.J. The complex radio spectrum of 3C 130. *Astron. Astrophys.* **1999**, *349*, 381–388.

47. Jetha, N.N.; Sakelliou, I.; Hardcastle, M.J.; Ponman, T.J.; Stevens, I.R. Interactions of radio galaxies and the intracluster medium in Abell 160 and Abell 2462. *Mon. Not. R. Astron. Soc.* **2005**, *358*, 1394–1404. [CrossRef]

48. Taylor, G.B.; Perley, R.A.; Inoue, M.; Kato, T.; Tabara, H.; Aizu, K. VLA Observations of the Radio Galaxy Hydra A (3C 218). *Astrophys. J.* **1990**, *360*, 41–54. [CrossRef]

49. Garon, A.F.; Rudnick, L.; Wong, O.I.; Jones, T.W.; Kim, J.A.; Andernach, H.; Shabala, S.S.; Kapińska, A.D.; Norris, R.P.; de Gasperin, F.; et al. Radio Galaxy Zoo: The Distortion of Radio Galaxies by Galaxy Clusters. *Astron. J.* **2019**, *157*, 126–143. [CrossRef]

50. Jetha, N.N.; Hardcastle, M.J.; Sakelliou, I. Jet speeds in wide-angle tailed radio galaxies. *Mon. Not. R. Astron. Soc.* **2006**, *368*, 609–618. [CrossRef]

51. Blandford, R.D.; Königl, A. Relativistic jets as compact radio sources. *Astrophys. J.* **1979**, *232*, 34–48. [CrossRef]

52. Venturi, T.; Castaldini, C.; Cotton, W.D.; Feretti, L.; Giovannini, G.; Lara, L.; Marcaide, J.M.; Wehrle, A.E. VLBI Observations of a Complete Sample of Radio Galaxies. VI. The Two FR I Radio Galaxies B2 0836+29 and 3C 465. *Astrophys. J.* **1995**, *454*, 735–744. [CrossRef]

53. Burns, J.O.; O'Dea, C.P.; Gregory, S.A.; Balonek, T.J. Observational Constraints on Bending the Wide-Angle Tailed Radio Galaxy 1919+479. *Astrophys. J.* **1986**, *307*, 73–90. [CrossRef]

54. Riley, J.M.; Branson, N.J.B.A. New observations of 3C 382, 3C 452 and 3C 465 at 2.7 and 5 GHz. *Mon. Not. R. Astron. Soc.* **1973**, *164*, 271–287. [CrossRef]

55. Feretti, L.; Giovannini, G.; Klein, U.; Mack, K.H.; Sijbring, L.G.; Zech, G. Electron ageing and polarization in tailed radio galaxies. *Astron. Astrophys.* **1998**, *331*, 475–484.

56. Young, A.; Rudnick, L.; Katz-Stone, D.M.; O'Donoghue, A.A. Electron population aging models for wide-angle tails. *New A Rev.* **2002**, *46*, 105–107. [CrossRef]

57. Eilek, J.A.; Owen, F.N. Magnetic Fields in Cluster Cores: Faraday Rotation in A400 and A2634. *Astrophys. J.* **2002**, *567*, 202–220. [CrossRef]

58. Burn, B.J. On the depolarization of discrete radio sources by Faraday dispersion. *Mon. Not. R. Astron. Soc.* **1966**, *133*, 67–83. [CrossRef]

59. Cioffi, D.F.; Jones, T.W. Internal Faraday rotation effects in transparent synchrotron sources. *Astron. J.* **1980**, *85*, 368–375. [CrossRef]

60. Lari, C.; Perola, G.C. Radio Properties of Abell Clusters. In *The Large Scale Structures in the Universe*; Longair, M.S., Einasto, J., Eds.; Springer: Dordrecht, The Netherlands, 1978; Volume 79, pp. 137–147.

61. Simon, A.J.B. Radio sources with complex morphologies in clusters of galaxies. *Mon. Not. R. Astron. Soc.* **1978**, *184*, 537–551. [CrossRef]

62. Valentijn, E.A. The distribution of some intrinsic parameters of head-tail radio sources. *Astron. Astrophys.* **1979**, *78*, 367–372.

63. Wing, J.D.; Blanton, E.L. Galaxy Cluster Environments of Radio Sources. *Astron. J.* **2011**, *141*, 88–112. [CrossRef]

64. Mao, M.Y.; Sharp, R.; Saikia, D.J.; Norris, R.P.; Johnston-Hollitt, M.; Middelberg, E.; Lovell, J.E.J. ATLAS, and Wide-Angle Tail Galaxies in ATLAS. *J. Astrophys. Astron.* **2011**, *32*, 585–588. [CrossRef]

65. Miraghaei, H.; Best, P.N. The nuclear properties and extended morphologies of powerful radio galaxies: The roles of host galaxy and environment. *Mon. Not. R. Astron. Soc.* **2017**, *466*, 4346–4363. [CrossRef]

66. Silverstein, E.M.; Anderson, M.E.; Bregman, J.N. Increased Prevalence of Bent Lobes for Double-lobed Radio Galaxies in Dense Environments. *Astron. J.* **2018**, *155*, 14–21. [CrossRef]
67. Liu, Y.X.; Xu, H.G.; Zheng, D.C.; Li, W.T.; Zhu, Z.H.; Ma, Z.X.; Lian, X.L. The environment of C- and S-shaped radio galaxies. *Res. Astron. Astrophys.* **2019**, *19*, 127–135. [CrossRef]
68. Pal, S.; Kumari, S. A new catalog of head-tail radio galaxies from LoTSS DR1. *J. Astrophys. Astron.* **2023**, *44*, 17–32. [CrossRef]
69. Golden-Marx, E.; Blanton, E.L.; Paterno-Mahler, R.; Brodwin, M.; Ashby, M.L.N.; Moravec, E.; Shen, L.; Lemaux, B.C.; Lubin, L.M.; Gal, R.R.; et al. The High-redshift Clusters Occupied by Bent Radio AGN (COBRA) Survey: Radio Source Properties. *Astrophys. J.* **2021**, *907*, 65–88. [CrossRef]
70. Morris, M.E.; Wilcots, E.; Hooper, E.; Heinz, S. How Does Environment Affect the Morphology of Radio AGN? *Astron. J.* **2022**, *163*, 280–294. [CrossRef]
71. Matthews, T.A.; Morgan, W.W.; Schmidt, M. A Discussion of Galaxies Indentified with Radio Sources. *Astrophys. J.* **1964**, *140*, 35–49. [CrossRef]
72. De Robertis, M.M.; Yee, H.K.C. Optical Nuclear Activity in the Radio Galaxy 3C 465. *Astron. J.* **1990**, *100*, 84–95. [CrossRef]
73. Buttiglione, S.; Capetti, A.; Celotti, A.; Axon, D.J.; Chiaberge, M.; Macchetto, F.D.; Sparks, W.B. An optical spectroscopic survey of the 3CR sample of radio galaxies with z < 0.3 . II. Spectroscopic classes and accretion modes in radio-loud AGN. *Astron. Astrophys.* **2010**, *509*, A6–A21. [CrossRef]
74. Blanton, E.L.; Gregg, M.D.; Helfand, D.J.; Becker, R.H.; Leighly, K.M. The Environments of a Complete Moderate-Redshift Sample of FIRST Bent-Double Radio Sources. *Astron. J.* **2001**, *121*, 2915–2927. [CrossRef]
75. Wing, J.D.; Blanton, E.L. An Examination of the Optical Substructure of Galaxy Clusters Hosting Radio Sources. *Astrophys. J.* **2013**, *767*, 102. [CrossRef]
76. Pinkney, J.; Rhee, G.; Burns, J.O.; Hill, J.M.; Oegerle, W.; Batuski, D.; Hintzen, P. The Dynamics of the Galaxy Cluster Abell 2634. *Astrophys. J.* **1993**, *416*, 36–50. [CrossRef]
77. Edwards, L.O.V.; Fadda, D.; Frayer, D.T. The First Bent Double Lobe Radio Source in a Known Cluster Filament: Constraints on the Intrafilament Medium. *Astrophys. J.* **2010**, *724*, L143–L147. [CrossRef]
78. Vardoulaki, E.; Vazza, F.; Jiménez-Andrade, E.F.; Gozaliasl, G.; Finoguenov, A.; Wittor, D. Bent It Like FRs: Extended Radio AGN in the COSMOS Field and Their Large-Scale Environment. *Galaxies* **2021**, *9*, 93. [CrossRef]
79. O'Brien, A.N.; Norris, R.P.; Tothill, N.F.H.; Filipović, M.D. The spatial correlation of bent-tail galaxies and galaxy clusters. *Mon. Not. R. Astron. Soc.* **2018**, *481*, 5247–5262. [CrossRef]
80. Burns, J.O. The structure and environment of the wide-angle tailed radio galaxy 1919+479. *Mon. Not. R. Astron. Soc.* **1981**, *195*, 523–533. [CrossRef]
81. Quintana, H.; Lawrie, D.G. On the determination of velocity dispersions for cD clusters of galaxies. *Astron. J.* **1982**, *87*, 1–6. [CrossRef]
82. White, S.D.M. The dynamics of rich clusters of galaxies. *Mon. Not. R. Astron. Soc.* **1976**, *177*, 717–733. [CrossRef]
83. White, S.D.M.; Rees, M.J. Core condensation in heavy halos: A two-stage theory for galaxy formation and clustering. *Mon. Not. R. Astron. Soc.* **1978**, *183*, 341–358. [CrossRef]
84. Beers, T.C.; Gebhardt, K.; Forman, W.; Huchra, J.P.; Jones, C. A Dynamical Analysis of Twelve Clusters of Galaxies. *Astron. J.* **1991**, *102*, 1581–1609. [CrossRef]
85. Gebhardt, K.; Beers, T.C. Bound Populations around cD Galaxies and cD Velocity Offsets in Clusters of Galaxies. *Astrophys. J.* **1991**, *383*, 72–89. [CrossRef]
86. Malumuth, E.M.; Kriss, G.A.; Dixon, W.V.D.; Ferguson, H.C.; Ritchie, C. Dynamics of Clusters of Galaxies with Central Dominant Galaxies. I. Galaxy Redshifts. *Astron. J.* **1992**, *104*, 495–530. [CrossRef]
87. Bird, C.M. Substructure in Clusters and Central Galaxy Peculiar Velocities. *Astron. J.* **1994**, *107*, 1637–1648. [CrossRef]
88. Oegerle, W.R.; Hill, J.M. Dynamics of cD Clusters of Galaxies. IV. Conclusion of a Survey of 25 Abell Clusters. *Astron. J.* **2001**, *122*, 2858–2873. [CrossRef]
89. Coziol, R.; Andernach, H.; Caretta, C.A.; Alamo-Martínez, K.A.; Tago, E. The Dynamical State of Brightest Cluster Galaxies and The Formation of Clusters. *Astron. J.* **2009**, *137*, 4795–4809. [CrossRef]
90. Beers, T.C.; Geller, M.J. The environment of D and cD galaxies. *Astrophys. J.* **1983**, *274*, 491–501. [CrossRef]
91. Zabludoff, A.I.; Mulchaey, J.S. The Properties of Poor Groups of Galaxies. I. Spectroscopic Survey and Results. *Astrophys. J.* **1998**, *496*, 39–72. [CrossRef]
92. Skibba, R.A.; van den Bosch, F.C.; Yang, X.; More, S.; Mo, H.; Fontanot, F. Are brightest halo galaxies central galaxies? *Mon. Not. R. Astron. Soc.* **2011**, *410*, 417–431. [CrossRef]
93. Martel, H.; Robichaud, F.; Barai, P. Major Cluster Mergers and the Location of the Brightest Cluster Galaxy. *Astrophys. J.* **2014**, *786*, 79. [CrossRef]
94. West, M.J.; Jones, C.; Forman, W. Substructure: Clues to the Formation of Clusters of Galaxies. *Astrophys. J.* **1995**, *451*, L5–L8. [CrossRef]
95. Burns, J.O. Stormy Weather in Galaxy Clusters. *Science* **1998**, *280*, 400–404. [CrossRef] [PubMed]
96. Burns, J.O.; Balonek, T.J. The curvature of radio jets and tails in the intracluster media of Abell 1446 and 2220. *Astrophys. J.* **1982**, *263*, 546–556. [CrossRef]

97. Burns, J.O.; Rhee, G.; Owen, F.N.; Pinkney, J. Clumped X-ray Emission around Radio Galaxies in Abell Clusters. *Astrophys. J.* **1994**, *423*, 94–115. [CrossRef]
98. Pinkney, J.; Burns, J.O.; Hill, J.M. 1919+479: Big WAT in a Poor Cluster. *Astron. J.* **1994**, *108*, 2031–2045. [CrossRef]
99. Gómez, P.L.; Pinkney, J.; Burns, J.O.; Wang, Q.; Owen, F.N.; Voges, W. ROSAT X-ray Observations of Abell Clusters with Wide-Angle Tailed Radio Sources. *Astrophys. J.* **1997**, *474*, 580–597. [CrossRef]
100. Gomez, P.L.; Ledlow, M.J.; Burns, J.O.; Pinkey, J.; Hill, J.M. The Cluster Dynamics, X-ray Emission, and Radio Galaxies in Abell 578 = Abell 1569. *Astron. J.* **1997**, *114*, 1711–1727. [CrossRef]
101. Schindler, S.; Prieto, M.A. X-ray analysis of Abell 2634 and its central galaxy 3C 465. *Astron. Astrophys.* **1997**, *327*, 37–46.
102. Sakelliou, I.; Merrifield, M.R.; McHardy, I.M. What bent the jets in 4C 34.16? *Mon. Not. R. Astron. Soc.* **1996**, *283*, 673–682. [CrossRef]
103. Sakelliou, I.; Merrifield, M.R. The distorted jets and gaseous environment of 3C 465. *Mon. Not. R. Astron. Soc.* **1999**, *305*, 417–424. [CrossRef]
104. Sakelliou, I.; Merrifield, M.R. The origin of wide-angle tailed radio galaxies. *Mon. Not. R. Astron. Soc.* **2000**, *311*, 649–656. [CrossRef]
105. Sakelliou, I.; Acreman, D.M.; Hardcastle, M.J.; Merrifield, M.R.; Ponman, T.J.; Stevens, I.R. The cool wake around 4C 34.16 as seen by XMM-Newton. *Mon. Not. R. Astron. Soc.* **2005**, *360*, 1069–1076. [CrossRef]
106. Novikov, D.I.; Melott, A.L.; Wilhite, B.C.; Kaufman, M.; Burns, J.O.; Miller, C.J.; Batuski, D.J. Cluster winds blow along supercluster axes. *Mon. Not. R. Astron. Soc.* **1999**, *304*, L5–L9. [CrossRef]
107. Douglass, E.M.; Blanton, E.L.; Clarke, T.E.; Sarazin, C.L.; Wise, M. Chandra Observation of the Cluster Environment of a WAT Radio Source in Abell 1446. *Astrophys. J.* **2008**, *673*, 763–777. [CrossRef]
108. Douglass, E. The Galaxy Cluster Environments of Wide Angle Tail Radio Sources. Ph.D. Thesis, Boston University, Boston, MA, USA, 2012.
109. Gómez, P.L.; Calderón, D. The Dynamics of the Wide-angle Tailed (WAT) Galaxy Cluster A562. *Astron. J.* **2020**, *160*, 152. [CrossRef]
110. Paterno-Mahler, R.; Blanton, E.L.; Randall, S.W.; Clarke, T.E. Deep Chandra Observations of the Extended Gas Sloshing Spiral in A2029. *Astrophys. J.* **2013**, *773*, 114. [CrossRef]
111. Paterno-Mahler, R.; Randall, S.W.; Bulbul, E.; Andrade-Santos, F.; Blanton, E.L.; Jones, C.; Murray, S.; Johnson, R.E. Merger Signatures in the Galaxy Cluster A98. *Astrophys. J.* **2014**, *791*, 104. [CrossRef]
112. Dasadia, S.; Sun, M.; Morandi, A.; Sarazin, C.; Clarke, T.; Nulsen, P.; Massaro, F.; Roediger, E.; Harris, D.; Forman, B. Shocking features in the merging galaxy cluster RXJ0334.2-0111. *Mon. Not. R. Astron. Soc.* **2016**, *458*, 681–694. [CrossRef]
113. Douglass, E.M.; Blanton, E.L.; Randall, S.W.; Clarke, T.E.; Edwards, L.O.V.; Sabry, Z.; ZuHone, J.A. The Megaparsec-scale Gas-sloshing Spiral in the Remnant Cool Core Cluster Abell 1763. *Astrophys. J.* **2018**, *868*, 121–141. [CrossRef]
114. Sarkar, A.; Randall, S.; Su, Y.; Alvarez, G.E.; Sarazin, C.L.; Jones, C.; Blanton, E.; Nulsen, P.; Chakraborty, P.; Bulbul, E.; et al. Gas Sloshing and Cold Fronts in Pre-merging Galaxy Cluster A98. *Astrophys. J.* **2023**, *944*, 132. [CrossRef]
115. Tiwari, J.; Singh, K.P. The complex intracluster medium of Abell 1569 and its interaction with central radio galaxies. *Mon. Not. R. Astron. Soc.* **2022**, *509*, 3321–3338. [CrossRef]
116. Clarke, T.E.; Blanton, E.L.; Sarazin, C.L. The Complex Cooling Core of A2029: Radio and X-ray Interactions. *Astrophys. J.* **2004**, *616*, 178–191. [CrossRef]
117. Pinkney, J. The Dynamics of Galaxy Clusters Containing Wide-Angle Tailed Radio Sources. Ph.D. Thesis, New Mexico State University, Las Cruces, NM, USA, 1995.
118. Pinkney, J.; Burns, J.O.; Ledlow, M.J.; Gómez, P.L.; Hill, J.M. Substructure in Clusters Containing Wide-Angle-Tailed Radio Galaxies. I. New Redshifts. *Astron. J.* **2000**, *120*, 2269–2277. [CrossRef]
119. Krempec-Krygier, J.; Krygier, B. Dynamics of the Abell 98 cluster and the radio structure of 4C+20.04. *Astron. Astrophys.* **1995**, *296*, 359–369.
120. Markevitch, M.; Vikhlinin, A. Shocks and cold fronts in galaxy clusters. *Phys. Rep.* **2007**, *443*, 1–53. [CrossRef]
121. Roettiger, K.; Burns, J.; Loken, C. When Clusters Collide: A Numerical Hydro/N-Body Simulation of Merging Galaxy Clusters. *Astrophys. J.* **1993**, *407*, L53–L56. [CrossRef]
122. Roettiger, K.; Burns, J.O.; Loken, C. The Observational Consequences of Merging Clusters of Galaxies. *Astrophys. J.* **1996**, *473*, 651–669. [CrossRef]
123. Roettiger, K.; Stone, J.M.; Mushotzky, R.F. Anatomy of a Merger: A Numerical Model of A754. *Astrophys. J.* **1998**, *493*, 62–72. [CrossRef]
124. Ricker, P.M.; Sarazin, C.L. Off-Axis Cluster Mergers: Effects of a Strongly Peaked Dark Matter Profile. *Astrophys. J.* **2001**, *561*, 621–644. [CrossRef]
125. Burns, J.O. The Radio Properties of cD Galaxies in Abell Clusters. I. an X-ray Selected Sample. *Astron. J.* **1990**, *99*, 14–30. [CrossRef]
126. Lewis, A.D.; Stocke, J.T.; Buote, D.A. Chandra Observations of Abell 2029: No Cooling Flow and a Steep Abundance Gradient. *Astrophys. J.* **2002**, *573*, L13–L17. [CrossRef]
127. David, L.P.; Kempner, J. Chandra and XMM-Newton Observations of the Double Cluster A1758. *Astrophys. J.* **2004**, *613*, 831–840. [CrossRef]

128. Russell, H.R.; Sanders, J.S.; Fabian, A.C.; Baum, S.A.; Donahue, M.; Edge, A.C.; McNamara, B.R.; O'Dea, C.P. Chandra observation of two shock fronts in the merging galaxy cluster Abell 2146. *Mon. Not. R. Astron. Soc.* **2010**, *406*, 1721–1733. [CrossRef]

129. Finoguenov, A.; Henriksen, M.J.; Briel, U.G.; de Plaa, J.; Kaastra, J.S. XMM-Newton Study of A3562 and Its Immediate Shapley Environs. *Astrophys. J.* **2004**, *611*, 811–820. [CrossRef]

130. ZuHone, J.A.; Markevitch, M.; Johnson, R.E. Stirring Up the Pot: Can Cooling Flows in Galaxy Clusters be Quenched by Gas Sloshing? *Astrophys. J.* **2010**, *717*, 908–928. [CrossRef]

131. ZuHone, J.A. A Parameter Space Exploration of Galaxy Cluster Mergers. I. Gas Mixing and the Generation of Cluster Entropy. *Astrophys. J.* **2011**, *728*, 54. [CrossRef]

132. Hahn, O.; Martizzi, D.; Wu, H.Y.; Evrard, A.E.; Teyssier, R.; Wechsler, R.H. rhapsody-g simulations—I. The cool cores, hot gas and stellar content of massive galaxy clusters. *Mon. Not. R. Astron. Soc.* **2017**, *470*, 166–186. [CrossRef]

133. Soker, N.; Sarazin, C.L. Cooling Flows and the Stability of Radio Jets. *Astrophys. J.* **1988**, *327*, 66–81. [CrossRef]

134. O'Dea, C.P.; Baum, S.A. Radio properties of central dominant galaxies in cluster cooling flows. *Natl. Radio Astron. Obs. Workshop* **1986**, *16*, 141–146.

135. Baum, S.A.; O'Dea, C.P. Multifrequency VLA observations of PKS 0745-191: The archetypal "cooling flow" radio source? *Mon. Not. R. Astron. Soc.* **1991**, *250*, 737. [CrossRef]

136. Blanton, E.L.; Randall, S.W.; Clarke, T.E.; Sarazin, C.L.; McNamara, B.R.; Douglass, E.M.; McDonald, M. A Very Deep Chandra Observation of A2052: Bubbles, Shocks, and Sloshing. *Astrophys. J.* **2011**, *737*, 99. [CrossRef]

137. Taylor, G.B.; O'Dea, C.P.; Peck, A.B.; Koekemoer, A.M. H I Absorption toward the Nucleus of the Radio Galaxy PKS 2322-123 in A2597. *Astrophys. J.* **1999**, *512*, L27–L30. [CrossRef]

138. Liuzzo, E.; Giovannini, G.; Giroletti, M.; Taylor, G.B. Parsec-scale properties of brightest cluster galaxies. *Astron. Astrophys.* **2010**, *516*, A1. [CrossRef]

139. Hintzen, P.; Ulvestad, J.; Owen, F. Are wide-angle radio-tail QSOs members of clusters of galaxies? I. VLA maps at 20 CM of 117 radio quasars. *Astron. J.* **1983**, *88*, 709–758. [CrossRef]

140. Blanton, E.L.; Gregg, M.D.; Helfand, D.J.; Becker, R.H.; White, R.L. Discovery of a High-Redshift (z = 0.96) Cluster of Galaxies Using a FIRST Survey Wide-Angle-Tailed Radio Source. *Astron. J.* **2003**, *125*, 1635–1641. [CrossRef]

141. Blanton, E.L.; Paterno-Mahler, R.; Wing, J.D.; Ashby, M.L.N.; Golden-Marx, E.; Brodwin, M.; Douglass, E.M.; Randall, S.W.; Clarke, T.E. Extragalactic jets as probes of distant clusters of galaxies and the clusters occupied by bent radio AGN (COBRA) survey. In *Proceedings of the Extragalactic Jets from Every Angle*; Massaro, F., Cheung, C.C., Lopez, E., Siemiginowska, A., Eds.; Cambridge University Press 2015; Volume 313, pp. 315–320. [CrossRef]

142. de Vries, W.H.; Becker, R.H.; White, R.L. Double-Lobed Radio Quasars from the Sloan Digital Sky Survey. *Astron. J.* **2006**, *131*, 666–679. [CrossRef]

143. Freeland, E.; Cardoso, R.F.; Wilcots, E. Bent-Double Radio Sources as Probes of Intergalactic Gas. *Astrophys. J.* **2008**, *685*, 858–862. [CrossRef]

144. Giacintucci, S.; Venturi, T. Tailed radio galaxies as tracers of galaxy clusters. Serendipitous discoveries with the GMRT. *Astron. Astrophys.* **2009**, *505*, 55–61. [CrossRef]

145. Oklopčić, A.; Smolčić, V.; Giodini, S.; Zamorani, G.; Bîrzan, L.; Schinnerer, E.; Carilli, C.L.; Finoguenov, A.; Lilly, S.; Koekemoer, A.; et al. Identifying Dynamically Young Galaxy Groups Via Wide-angle Tail Galaxies: A Case Study in the COSMOS Field at z = 0.53. *Astrophys. J.* **2010**, *713*, 484–490. [CrossRef]

146. Oklopčić, A.; Smolčić, V.; Giodini, S.; Zamorani, G.; Bhatirzan, L.; Schinnerer, E.; Carilli, C.L.; Finoguenov, A.; Lilly, S.; Koekemoer, A.; et al. A wide-angle tail galaxy at z = 0.53 in the COSMOS field. *Mem. Della Soc. Astron. Ital.* **2011**, *82*, 161.

147. Mao, M.Y.; Sharp, R.; Saikia, D.J.; Norris, R.P.; Johnston-Hollitt, M.; Middelberg, E.; Lovell, J.E.J. Wide-angle tail galaxies in ATLAS. *Mon. Not. R. Astron. Soc.* **2010**, *406*, 2578–2590. [CrossRef]

148. Banfield, J.K.; Andernach, H.; Kapińska, A.D.; Rudnick, L.; Hardcastle, M.J.; Cotter, G.; Vaughan, S.; Jones, T.W.; Heywood, I.; Wing, J.D.; et al. Radio Galaxy Zoo: Discovery of a poor cluster through a giant wide-angle tail radio galaxy. *Mon. Not. R. Astron. Soc.* **2016**, *460*, 2376–2384. [CrossRef]

149. Paterno-Mahler, R.; Blanton, E.L.; Brodwin, M.; Ashby, M.L.N.; Golden-Marx, E.; Decker, B.; Wing, J.D.; Anand, G. The High-redshift Clusters Occupied by Bent Radio AGN (COBRA) Survey: The Spitzer Catalog. *Astrophys. J.* **2017**, *844*, 78. [CrossRef]

150. Golden-Marx, E.; Blanton, E.L.; Paterno-Mahler, R.; Brodwin, M.; Ashby, M.L.N.; Lemaux, B.C.; Lubin, L.M.; Gal, R.R.; Tomczak, A.R. The High-redshift Clusters Occupied by Bent Radio AGN (COBRA) Survey: Follow-up Optical Imaging. *Astrophys. J.* **2019**, *887*, 50–90. [CrossRef]

151. Freeland, E.; Wilcots, E. Intergalactic Gas in Groups of Galaxies: Implications for Dwarf Spheroidal Formation and the Missing Baryons Problem. *Astrophys. J.* **2011**, *738*, 145. [CrossRef]

152. Bhukta, N.; Mondal, S.K.; Pal, S. Tailed radio galaxies from the TIFR GMRT sky survey. *Mon. Not. R. Astron. Soc.* **2022**, *516*, 372–390. [CrossRef]

153. Dehghan, S.; Johnston-Hollitt, M.; Franzen, T.M.O.; Norris, R.P.; Miller, N.A. Bent-tailed Radio Sources in the Australia Telescope Large Area Survey of the Chandra Deep Field South. *Astron. J.* **2014**, *148*, 75. [CrossRef]

154. Norris, R.P.; Hopkins, A.M.; Afonso, J.; Brown, S.; Condon, J.J.; Dunne, L.; Feain, I.; Hollow, R.; Jarvis, M.; Johnston-Hollitt, M.; et al. EMU: Evolutionary Map of the Universe. *Publ. Astron. Soc. Aust.* **2011**, *28*, 215–248. [CrossRef]

155. Mguda, Z.; Faltenbacher, A.; Heyden, K.v.d.; Gottlöber, S.; Cress, C.; Vaisanen, P.; Yepes, G. Ram pressure statistics for bent tail radio galaxies. *Mon. Not. R. Astron. Soc.* **2015**, *446*, 3310–3318. [CrossRef]
156. Proctor, D.D. Morphological Annotations for Groups in the First Database. *Astrophys. J. Suppl. Ser.* **2011**, *194*, 31. [CrossRef]
157. Croston, J.H.; Hardcastle, M.J.; Mingo, B.; Best, P.N.; Sabater, J.; Shimwell, T.M.; Williams, W.L.; Duncan, K.J.; Röttgering, H.J.A.; Brienza, M.; et al. The environments of radio-loud AGN from the LOFAR Two-Metre Sky Survey (LoTSS). *Astron. Astrophys.* **2019**, *622*, A10. [CrossRef]
158. Proctor, D.D. Comparing Pattern Recognition Feature Sets for Sorting Triples in the FIRST Database. *Astrophys. J. Suppl. Ser.* **2006**, *165*, 95–107. [CrossRef]
159. Burns, J.O.; Gregory, S.A. The structure of 4C radio galaxies in poor clusters. *Astron. J.* **1982**, *87*, 1245–1265. [CrossRef]
160. Hardcastle, M.J.; Sakelliou, I.; Worrall, D.M. A Chandra and XMM-Newton study of the wide-angle tail radio galaxy 3C465. *Mon. Not. R. Astron. Soc.* **2005**, *359*, 1007–1021. [CrossRef]
161. O'Dea, C.P.; Owen, F.N. VLA observations of 57 sources in clusters of galaxies. *Astron. J.* **1985**, *90*, 927–953. [CrossRef]
162. O'Dea, C.P.; Owen, F.N. Multifrequency VLA Observations of the Prototypical Narrow-Angle Tail Radio Source, NGC 1265. *Astrophys. J.* **1986**, *301*, 841–859. [CrossRef]
163. Norman, M.L.; Burns, J.O.; Sulkanen, M.E. Disruption of galactic radio jets by shocks in the ambient medium. *Nature* **1988**, *335*, 146–149. [CrossRef]
164. Loken, C.; Roettiger, K.; Burns, J.O.; Norman, M. Radio Jet Propagation and Wide-Angle Tailed Radio Sources in Merging Galaxy Cluster Environments. *Astrophys. J.* **1995**, *445*, 80–97. [CrossRef]
165. Appl, S.; Lery, T.; Baty, H. Current-driven instabilities in astrophysical jets. Linear analysis. *Astron. Astrophys.* **2000**, *355*, 818–828.
166. Hardee, P.E. The stability of astrophysical jets. In *Proceedings of the Jets at All Scales*; Romero, G.E., Sunyaev, R.A., Belloni, T., Eds.; Cambridge University Press 2011; Volume 275, pp. 41–49. [CrossRef]
167. Massaglia, S.; Bodo, G.; Rossi, P.; Capetti, S.; Mignone, A. Making Faranoff-Riley I radio sources. II. The effects of jet magnetization. *Astron. Astrophys.* **2019**, *621*, A132. [CrossRef]
168. Martí, J.M. Numerical Simulations of Jets from Active Galactic Nuclei. *Galaxies* **2019**, *7*, 24. [CrossRef]
169. Barniol Duran, R.; Tchekhovskoy, A.; Giannios, D. Simulations of AGN jets: Magnetic kink instability versus conical shocks. *Mon. Not. R. Astron. Soc.* **2017**, *469*, 4957–4978. [CrossRef]
170. Massaglia, S.; Bodo, G.; Rossi, P.; Capetti, A.; Mignone, A. Making Fanaroff-Riley I radio sources. III. The effects of the magnetic field on relativistic jets' propagation and source morphologies. *Astron. Astrophys.* **2022**, *659*, A139. [CrossRef]
171. Chen, Y.H.; Heinz, S.; Hooper, E. A Numerical Study of the Impact of Jet Magnetic Topology on Radio Galaxy Evolution. *arXiv* **2023**, arXiv:2304.03863. https://doi.org/10.48550/arXiv.2304.03863.
172. Gan, Z.; Li, H.; Li, S.; Yuan, F. Three-dimensional Magnetohydrodynamical Simulations of the Morphology of Head-Tail Radio Galaxies Based on the Magnetic Tower Jet Model. *Astrophys. J.* **2017**, *839*, 14. [CrossRef]
173. Hardee, P.E. Spatial Stability of Relativistic Jets: Application to 3C 345. *Astrophys. J.* **1987**, *318*, 78–92. [CrossRef]
174. Birkinshaw, M. The Kelvin-Helmholtz instability for relativistic particle beams—II. Flows bounded by a simple shear layer. *Mon. Not. R. Astron. Soc.* **1991**, *252*, 505. [CrossRef]
175. Birkinshaw, M. Instabilities in Astrophysical Jets. *Astrophys. Space Sci.* **1996**, *242*, 17–91. [CrossRef]
176. Hamlin, N.D.; Newman, W.I. Role of the Kelvin-Helmholtz instability in the evolution of magnetized relativistic sheared plasma flows. *Phys. Rev. E* **2013**, *87*, 043101. [CrossRef]
177. Gopal-Krishna.; Wiita, P.J. The expansion and cosmological evolution of powerful radio sources. *Mon. Not. R. Astron. Soc.* **1987**, *226*, 531–542. [CrossRef]
178. Hooda, J.S.; Wiita, P.J. Three-dimensional Simulations of Extragalactic Jets Crossing Interstellar Medium/Intracluster Medium Interfaces. *Astrophys. J.* **1996**, *470*, 211–221. [CrossRef]
179. Zhang, H.M.; Koide, S.; Sakai, J.I. Two-Dimensional Simulations of Relativistic Extragalactic Jets Crossing an ISM/ICM Interface. *PASJ* **1999**, *51*, 449–457. [CrossRef]
180. Hardee, P.E.; White, Raymond E., I.; Norman, M.L.; Cooper, M.A.; Clarke, D.A. Asymmetric Morphology of the Propagating Jet. II. The Effect of Atmospheric Gradients. *Astrophys. J.* **1992**, *387*, 460–483. [CrossRef]
181. Higgins, S.W.; O'Brien, T.J.; Dunlop, J.S. Structures produced by the collision of extragalactic jets with dense clouds. *Mon. Not. R. Astron. Soc.* **1999**, *309*, 273–286. [CrossRef]
182. Wang, Z.; Wiita, P.J.; Hooda, J.S. Radio Jet Interactions with Massive Clouds. *Astrophys. J.* **2000**, *534*, 201–212. [CrossRef]
183. Wiita, P.J. Jet Propagation Through Irregular Media and the Impact of Lobes on Galaxy Formation. *ApSS* **2004**, *293*, 235–245. .:ASTR.0000044672.94932.c5. [CrossRef]
184. O'Dea, C.P.; Owen, F.N.; Keel, W.C. Optical spectroscopy of radio jets in 3C 31, 3C 75, 3C 83.1B, and 3C 465. *Can. J. Phys.* **1986**, *64*, 369–372. [CrossRef]
185. O'Dea, C.P.; Saikia, D.J. Compact steep-spectrum and peaked-spectrum radio sources. *Astron. Astrophys.r* **2021**, *29*, 3. [CrossRef]
186. Gull, S.F.; Northover, K.J.E. Bubble Model of Extragalactic Radio Sources. *Nature* **1973**, *244*, 80–83. [CrossRef]
187. Cowie, L.L.; McKee, C.F. A dynamical model of the tailed radio galaxies. *Astron. Astrophys.* **1975**, *43*, 337–343.
188. Worrall, D.M.; Birkinshaw, M.; Cameron, R.A. The X-ray Environment of the Dumbbell Radio Galaxy NGC 326. *Astrophys. J.* **1995**, *449*, 93. [CrossRef]
189. Laing, R.A. Magnetic fields in extragalactic radio sources. *Astrophys. J.* **1981**, *248*, 87–104. [CrossRef]

190. Benford, G. Current-carrying beams in astrophysics: Models for double radio sources and jets. *Mon. Not. R. Astron. Soc.* **1978**, *183*, 29–48. [CrossRef]

191. Chan, K.L.; Henriksen, R.N. On the supersonic dynamics of magnetized jets of thermal gas in radio galaxies. *Astrophys. J.* **1980**, *241*, 534–551. [CrossRef]

192. Heyvaerts, J.; Norman, C. The Collimation of Magnetized Winds. *Astrophys. J.* **1989**, *347*, 1055. [CrossRef]

193. Lynden-Bell, D. On why discs generate magnetic towers and collimate jets. *Mon. Not. R. Astron. Soc.* **2003**, *341*, 1360–1372. [CrossRef]

194. Gabuzda, D. Evidence for Helical Magnetic Fields Associated with AGN Jets and the Action of a Cosmic Battery. *Galaxies* **2018**, *7*, 5. [CrossRef]

195. Fendt, C.; Zinnecker, H. Possible bending mechanisms of protostellar jets. *Astron. Astrophys.* **1998**, *334*, 750–755.

196. Burns, J.O.; Loken, C.; Roettiger, K.; Rizza, E.; Bryan, G.; Norman, M.L.; Gómez, P.; Owen, F.N. Stormy weather and cluster radio galaxies. *New A Rev.* **2002**, *46*, 135–140. [CrossRef]

197. Mendygral, P.J.; Jones, T.W.; Dolag, K. MHD Simulations of Active Galactic Nucleus Jets in a Dynamic Galaxy Cluster Medium. *Astrophys. J.* **2012**, *750*, 166. [CrossRef]

198. Landau, L.D.; Lifshitz, E.M. *Fluid Mechanics*; Pergamon Press: Oxford, UK, 1959.

199. Patnaik, A.R.; Banhatti, D.G.; Subrahmanya, C.R. VLA observations of the wide-angle tailed radio source 1313+073. *Mon. Not. R. Astron. Soc.* **1984**, *211*, 775–781. [CrossRef]